

Surface-plasmon-polariton mode conversion on rough interfaces

J. Giergiel and C. E. Reed*

Department of Physics, University of California, Irvine, California 92717

J. C. Hemminger

Department of Chemistry, University of California, Irvine, California 92717

S. Ushioda

Research Institute of Electrical Communication, Tohoku University, Sendai 980, Japan

(Received 3 November 1986)

We have observed mode conversion in the structure that supports two surface-plasmon polaritons. This mode-conversion phenomenon shows up as the emission from *both* modes, when either of the modes is excited, and is due to intrinsic roughness of the interfaces. We present an outline of a first-order (in roughness) Green's-function-based theory that yields a simple expression for the scattering cross section and which is in good agreement with the experimental data. Implications of these results for light-emitting tunnel junctions are discussed.

INTRODUCTION

Surface-plasmon polaritons (SPP) have been found to play important roles in optical processes involving metallic surfaces. In the case of surface-enhanced Raman scattering (SERS),¹ their resonant excitation by the incident laser beam generates strongly enhanced electric fields near metal surfaces and causes at least part of the enhancement of Raman scattering by adsorbed molecules²⁻⁵ (the so-called "electromagnetic effect" in SERS). The same effect also results in enhanced second-harmonic generation (SHG) at the metal surface.⁶ In the case of light-emitting tunnel junctions (LETJ), SPP are excited by tunneling currents and they in turn emit external light.^{7,8} The SPP on a perfectly flat metal surface are nonradiative;⁹ thus to facilitate radiative decay of SPP into external light, one must roughen the surface or draw a grating on the tunnel-junction surface to break the conservation of wave vectors k_{\parallel} parallel to the surface. Or one can provide coupling by a prism as was demonstrated recently by one of us.¹⁰ In Ref. 10 it was suggested that the slow mode of the tunnel junction is being converted to the fast mode which is radiative in the coupler prism. This cross coupling or mode conversion was assumed to occur due to residual roughness of the junction. More recently, Gruhlke, Holland, and Hall¹¹ have demonstrated the existence of mode coupling between the two SPP modes that propagate on the opposite sides of a silver film. On the theoretical side, Weber and Mills¹² presented a theory of cross coupling between different modes of SPP in a metal film. This is the background through which we have come to focus our attention on the question of mode conversion among different modes of SPP in thin metal films.

In this paper we present an outline of a physically appealing theory of mode coupling or conversion between two SPP modes of a thin-metal film via surface roughness, and demonstrate the applicability of the theory to experimental results. The main purpose of this paper is to show that a qualitatively satisfactory theory of mode conversion

can be formulated and that it agrees well with actual measurements. Thus, we will defer the detailed derivation to another paper¹³ dedicated to the theory, and in this paper we will concentrate on the comparison of theoretical results with experimental results.

Consider the sample geometry shown in Fig. 1, consisting of a hemispherical glass prism ($\epsilon_p = 2.3$), an MgF_2 film ($\epsilon \cong 1.9$) and an Ag film. The Ag film is bounded by vacuum and the MgF_2 film; thus, there are two modes of SPP arising from the two inequivalent in-

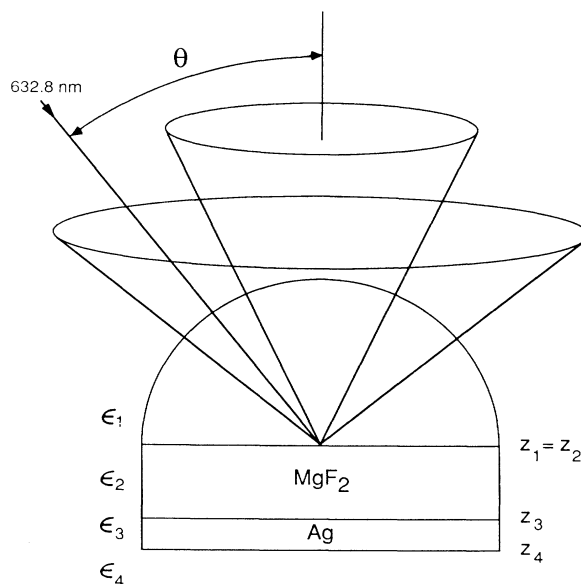


FIG. 1. Sample and experimental geometry. The cones represent light emitted by the two surface-plasmon polaritons of the silver film. The angle of emission is determined by the mode dispersion relations. The intensity of emission is monitored by two p - i - n photodiodes positioned on the cones in the plane perpendicular to the plane of incidence. The p -polarized laser beam can excite either of the modes depending on the angle of incidence.

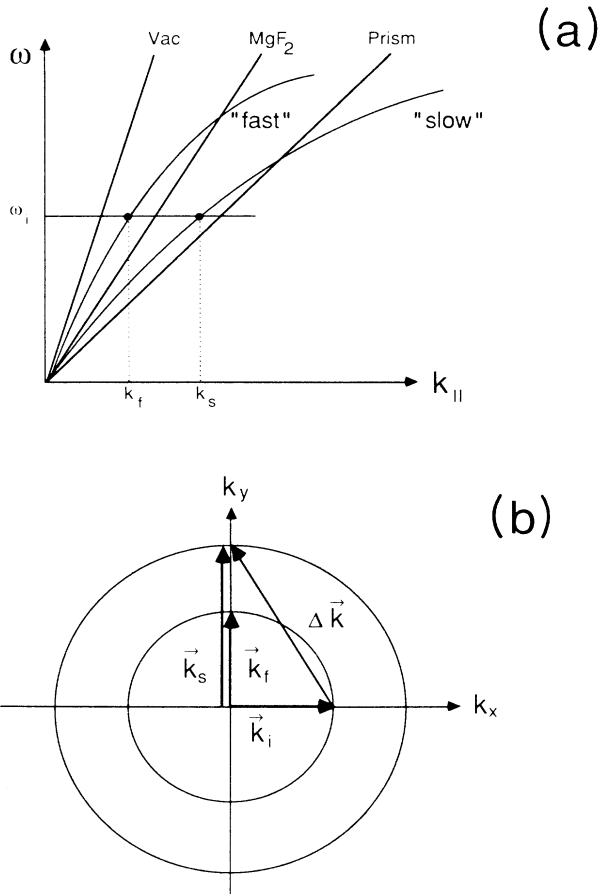


FIG. 2. (a) Schematic representation of the dispersion relation for the two SPP's supported by silver film in Fig. 1. The straight lines are the light lines in the various media. (b) The relationship among the wave vectors in the plane of the film.

terfaces of the Ag film. The mode structure (dispersion curves) of this layered structure is schematically shown in Fig. 2(a). The "fast" mode is predominantly localized at the Ag/vacuum interface and the "slow" mode is similarly localized at the MgF₂/Ag interface. Since the dielectric constant of BK7 glass (Schott Optical Glass Inc.) is greater than that of the MgF₂ film, a portion of both of these modes lie to the left of the light line in the prism. Thus, both the slow and the fast modes are radiative in the prism. Consequently, when one shines a beam of light through the prism at appropriate angles of incidence θ , either of the modes can be excited; i.e., when

$$k_{\parallel} = \frac{(\epsilon_p)^{1/2} \omega}{c} \sin \theta = k_s \text{ or } k_f, \quad (1)$$

where k_s and k_f are the wave vectors of the respective modes at frequency ω as shown in Fig. 2(a).

Now the question we ask is as follows: in the presence of surface roughness, how much of the energy injected into either mode at k_s or k_f is converted to the other mode or the same mode with a different k_{\parallel} vector? Figure 2(b) shows the wave-vector relations in the plane of the

surface. k_i is the parallel component of the wave vector of the incident light, and we observe the radiation emitted 90° away in the azimuthal direction from k_i . In our experiment two detectors were located in the directions corresponding to k_s and k_f in Fig. 2(b). Thus, one detector measures emission from the slow mode with wave vector k_s and the second detector measures emission from the fast mode at k_f . In what follows we will call these detectors "slow-mode detector" and "fast-mode detector," respectively. The emission intensities were measured by the two detectors as the magnitude of k_{\parallel} was varied over the range covering both k_s and k_f . As we describe later, when either of the modes is excited both modes radiate light into the detectors, showing that mode conversion is taking place.

In the following sections we will present the outline of a Green's-function theory that describes mode conversion via small surface roughness, and then describe the details of the experiment.

THEORETICAL MODEL

The scattering of light by rough interfaces has been considered by numerous authors. Various formalisms have been used, ranging from a relatively simple Fresnel-coefficient-type approach¹⁴ to a more general apparatus of electromagnetic Green's functions.^{15,16} Most of the authors considered specific experimental geometries, with only one [Bousquet *et al.* (Ref. 17)] presenting a full theoretical treatment extended to a general case of an arbitrary multilayer stack. In what follows, we outline a formalism that is based on the electromagnetic Green's function and which was generalized to an arbitrary number of layers. Such generalization is possible because of a certain symmetry property these functions have to satisfy with respect to the location of source and observation points. This symmetry property and the method of evaluation of the Green's functions for an arbitrary stack is fully discussed in our recent paper (Ref. 18). As in all previous treatments, we treat roughness in a first-order approximation, this being justified by a relative weakness of the roughness-induced scattering. In the final formulas for intensity of scattered light, the roughness enters through its statistical properties including a cross-correlation term that describes a degree to which profiles of various interfaces are related to each other.

We consider an arbitrary stack (Fig. 3) of n dielectric layers each described by a local, linear, and isotropic dielectric constant ϵ_i and of unit magnetic permeability μ . The layers are separated by rough boundaries located at $z = z_i(\mathbf{x})$, where \mathbf{x} is a vector in the x - y plane. Since the actual profile of a rough interface is never known, $z_i(\mathbf{x})$ will be considered a random stochastic process. We introduce a nominal planar boundary located at z_i , such that $\langle z_i(\mathbf{x}) - z_i \rangle \equiv \langle \zeta_i(\mathbf{x}) \rangle = 0$, where angular brackets denote averaging over all possible interface profiles. The deviation of the profile from the nominal boundary position is assumed to be very small. The geometry of Fig. 3 and the following theoretical treatment is a generalization of simpler geometries previously considered by Laks and Mills¹⁵ and Mills and Maradudin.¹⁶

Electromagnetic properties of this geometry are given

by a set of Green's functions $D_{\alpha\beta}(\mathbf{r}, \mathbf{r}')$ in the sense that once a driving current $\mathbf{J}(\mathbf{r}')$ is known, the electric fields can be calculated everywhere by the equation

$$E_{\alpha}(\mathbf{r}) = -\frac{i\omega}{c^2} \sum_{\beta} \int d^3r' D_{\alpha\beta}(\mathbf{r}, \mathbf{r}') J_{\beta}(\mathbf{r}') . \quad (2)$$

Here, subscripts α and β take on values x , y , and z . The full Green's functions $D_{\alpha\beta}(\mathbf{r}, \mathbf{r}')$ can be represented by a sum of Green's functions for a stack with perfectly smooth interfaces $D_{\alpha\beta}^0(\mathbf{r}, \mathbf{r}')$ and the correction term, $D'_{\alpha\beta}(\mathbf{r}, \mathbf{r}')$, due to the presence of roughness:

$$D_{\alpha\beta}(\mathbf{r}, \mathbf{r}') = D_{\alpha\beta}^0(\mathbf{r}, \mathbf{r}') + D'_{\alpha\beta}(\mathbf{r}, \mathbf{r}') . \quad (3)$$

The Green's functions for the smooth stack are known and can be used to obtain a first-order approximation to the full Green's function. The correction term, which is responsible for mode conversion, is given by

$$D'_{\alpha\beta}(\mathbf{r}, \mathbf{r}') = -\frac{\omega^2}{4\pi c^2} \sum_{\gamma} \int d^3r'' [\epsilon(\mathbf{r}'') - \epsilon^0(\mathbf{r}'')] \times D_{\alpha\gamma}^0(\mathbf{r}, \mathbf{r}'') D_{\gamma\beta}(\mathbf{r}'', \mathbf{r}') ,$$

where $\epsilon(\mathbf{r})$ includes the effect of rough boundaries and $\epsilon^0(\mathbf{r})$ is the dielectric constant of a perfectly smooth stack. Application of the Rayleigh hypothesis together with the assumption of small roughness yields a first-order approximation.¹⁵

$$D'_{\alpha\beta}(\mathbf{r}, \mathbf{r}') \cong -\frac{\omega^2}{4\pi c^2} \sum_{i=2}^n (\epsilon_i - \epsilon_{i-1}) \sum_{\gamma} \int d^2x'' D_{\alpha\gamma}^0(\mathbf{x}, \mathbf{x}'', z, z_i^+) D_{\gamma\beta}^0(\mathbf{x}'', \mathbf{x}', z_i^-, z') \zeta_i(\mathbf{x}'') , \quad (4)$$

where $z_i^{\pm} = z_i \pm \delta$ and δ is a small positive quantity. The physical contents of Eq. (4) can be better appreciated by writing an explicit expression for the amplitude of the scattered fields:

$$E_{\alpha}(\mathbf{r}) \simeq -\frac{i\omega}{c^2} \times \sum_{i=2}^n \sum_{\gamma} \int d^2x'' D_{\alpha\gamma}^0(\mathbf{x}, \mathbf{x}'', z, z_i^+) J_{\gamma}^{\text{sc}}(\mathbf{x}'', z_i^+) ,$$

where

$$J_{\gamma}^{\text{sc}}(\mathbf{x}'', z) = -\frac{\omega^2}{4\pi c^2} \zeta_i(\mathbf{x}'') (\epsilon_i - \epsilon_{i-1}) \times \sum_{\beta} \int d^3r' D_{\gamma\beta}^0(\mathbf{x}'', \mathbf{x}', z, z') J_{\beta}(\mathbf{r}') . \quad (5)$$

Thus, the scattered field is due to a set of current sheets $J^{\text{sc}}(\mathbf{x}'', z_i^+)$ localized in the roughness region of the stack

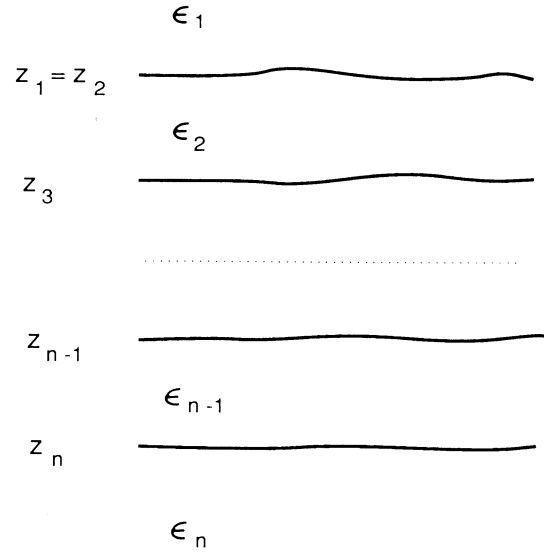
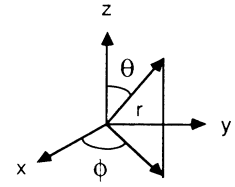


FIG. 3. An arbitrary stack of dielectric layers with rough interfaces. The z direction is normal to the stack.

and radiating as if no roughness was present. These roughness-generated current sheets are proportional to $\zeta_i(\mathbf{x})$ and to the difference between currents generated on two sides of a perfectly smooth interface by an external current source $\mathbf{J}(\mathbf{r}')$. Such a sheet current source was in fact a starting point in the early treatment of light scattering from rough planar interfaces given by Kröger and Kretschmann.¹⁴

As will be shown in Ref. 13, Eq. (5) leads to rather simple expressions for scattering cross sections. The scattering cross section is defined as the power radiated in the direction (θ, ϕ) , per unit solid angle, per unit incident flux in the direction (θ', ϕ') . The scattering cross section thus defined determines the conversion rate or cross-coupling rate between the modes separated in the \mathbf{k}_{\parallel} space by $\Delta\mathbf{k} \equiv \mathbf{k}_{\text{sc}} - \mathbf{k}_I$ where \mathbf{k}_{sc} is the wave vector of the scattered mode in the plane. For the four possible combinations of incident and scattered light polarization, the cross sections are given by

$$\sigma_{p \rightarrow p} = \frac{\omega^4}{(4\pi)^2 c^4} \left| \sum_{i=2}^n (\epsilon_i - \epsilon_{i-1}) \zeta_i(\Delta\mathbf{k}) E_z^p(\mathbf{k}_{\text{sc}}, z_i^+) E_z^p(\mathbf{k}_I, z_i^-) + \cos(\phi - \phi') E_{\parallel}^p(\mathbf{k}_{\text{sc}}, z_i^+) E_{\parallel}^p(\mathbf{k}_I, z_i^-) \right|^2 , \quad (6a)$$

$$\sigma_{s \rightarrow p} = \frac{\omega^4}{(4\pi)^2 c^4} \left| \sum_{i=2}^n (\epsilon_i - \epsilon_{i-1}) \zeta_i(\Delta \mathbf{k}) E_{\parallel}^p(\mathbf{k}_{sc}, z_i^+) E_{\parallel}^s(\mathbf{k}_I, z_i^-) \right|^2 \sin^2(\phi - \phi'), \quad (6b)$$

$$\sigma_{p \rightarrow s} = \frac{\omega^4}{(4\pi)^2 c^4} \left| \sum_{i=2}^n (\epsilon_i - \epsilon_{i-1}) \zeta_i(\Delta \mathbf{k}) E_{\parallel}^s(\mathbf{k}_{sc}, z_i^+) E_{\parallel}^p(\mathbf{k}_I, z_i^-) \right|^2 \sin^2(\phi - \phi'), \quad (6c)$$

$$\sigma_{s \rightarrow s} = \frac{\omega^4}{(4\pi)^2 c^4} \left| \sum_{i=2}^n (\epsilon_i - \epsilon_{i-1}) \zeta_i(\Delta \mathbf{k}) E_{\parallel}^s(\mathbf{k}_{sc}, z_i^+) E_{\parallel}^s(\mathbf{k}_I, z_i^-) \right|^2 \cos^2(\phi - \phi'). \quad (6d)$$

Here, we assumed that both the source and the detector are far away from the stack $|\mathbf{r}|, |\mathbf{r}'| \rightarrow \infty$. In Eqs. (6a)–(6d), k_I and k_{sc} are in-plane ($x-y$) components of wave vectors of incident and scattered radiation,

$$\mathbf{k}_I = (\epsilon_i)^{1/2} (\omega/c) \sin\theta' (\cos\phi', \sin\phi', 0),$$

$$\mathbf{k}_{sc} = (\epsilon_{sc})^{1/2} (\omega/c) \sin\theta (\cos\phi, \sin\phi, 0),$$

and $\zeta_i(\mathbf{k})$ is a Fourier component of $\zeta_i(\mathbf{x})$. $E_{\parallel}^s(k, z)$, $E_{\parallel}^p(k, z)$, and $E_{\parallel}^p(k, z)$ are the components of electric fields at location z due, respectively, to s - and p -polarized, unit-amplitude plane waves incident upon the perfectly smooth stack. Physically, $E(k, z)$ reflect the “efficiency” with which external sources generate fields within the structure. For p -polarized fields, the $E(k_I z)$ factor has strong resonances whenever k corresponds to one of the normal modes of the structure. Note that we have both $E(k_I)$ and $E(k_{sc})$ in the preceding equations. The first is obviously related to incident radiation, it determines field strength at the rough interface. The second which physically must correspond to the efficiency with which roughness-induced current radiates energy out is given by $E(k_{sc})$, the “efficiency” of the reverse process. That this is so follows quite generally from the Lorentz reciprocity theorem.^{18,19}

From Eqs. (6a) and (6b) it is clear that the cross section will have a rather pronounced maximum when both k_{sc} and k_I are the wave vectors of resonant modes of the dielectric stack. Since as we mentioned before the metal film can support only transverse magnetic modes (equivalent to p polarization), we expect only the $\sigma(p \rightarrow p)$ cross section to exhibit a strong maximum.

EXPERIMENT

Figure 1 shows the sample and experimental geometry used in this work. The sample was a hemispherical glass prism (BK7: $\epsilon_p = 2.3$) coated with an MgF_2 spacer of thickness 260 nm and a 46-nm Ag film on top. Both films were prepared by evaporation in a standard liquid-nitrogen-trapped, diffusion-pumped vacuum system at pressures in the 10^{-5} -Pa (10^{-7} -Torr) range. The glass prism was at room temperature and the Ag evaporation followed MgF_2 evaporation without a break in vacuum. The surface roughness that is responsible for the mode conversion was not introduced intentionally, but it is present naturally from the evaporation process.

A 632.8-nm laser beam was used to excite directly one of the modes by rotating the prism so that the incident angle satisfies Eq. (1). The beam was p -polarized and col-

limited inside the prism with the help of a lens. Two p - i - n photodiodes measure light scattered into two polar angles corresponding to two surface-plasmon polaritons in the plane normal to the plane of incidence. Light that reaches the detectors is due to a scattering process depicted in Fig. 2(b). The two circles represent the magnitudes of the wave vectors of the two surface-plasmon polaritons supported by a silver film at a fixed frequency corresponding to the wavelength of 632.8 nm. With the incident beam driving the fast mode directly (the situation depicted in the figure), the slow detector detects conversion of the driven fast mode into the slow one. The other detector (fast) records scattering of the fast mode into another fast mode propagating at 90° with respect to the original direction of propagation (\mathbf{k}_I). The experimental data (see Figs. 4 and 5) clearly demonstrate that these two processes occur simultaneously. For example, when the angle of incidence is $\sim 43.2^\circ$, which corresponds to the direct excitation of the fast mode, both the slow- and the fast-mode detector show an increase in the scattered intensity. A similar effect is observed at 83.4° angle of incidence when the slow mode is driven. Note the Fano-type line shape of the slow- to fast mode conversion process. This feature of the data is fully accounted for by the theory, and as we show below reflects the fact that the mode conversion occurs at all rough boundaries of the stack.

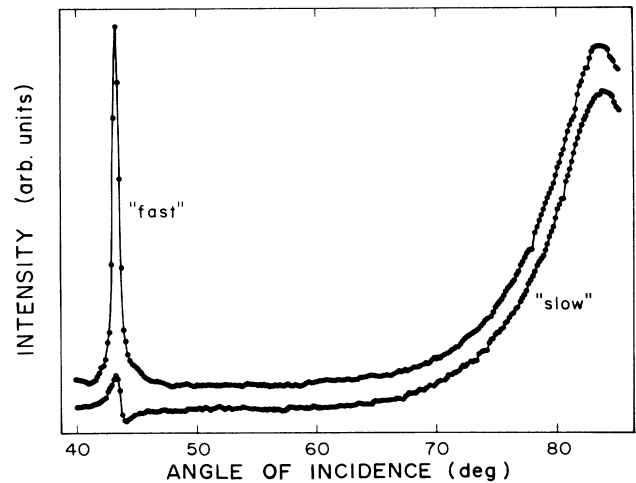


FIG. 4. The intensity of emission into (a) the fast mode and (b) the slow mode as a function of the angle of incidence.

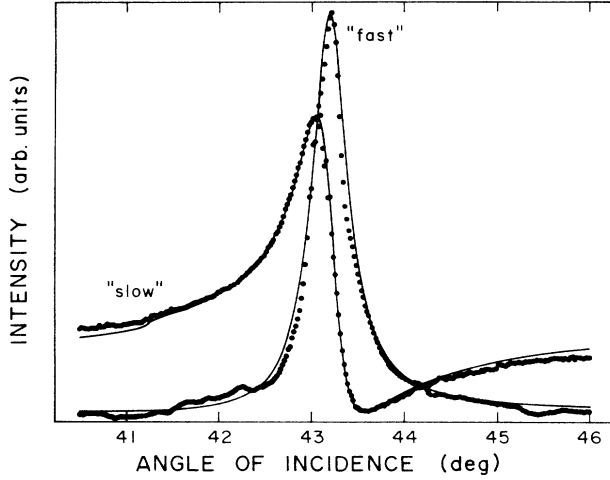


FIG. 5. The experimental data and the theoretical fit in the region of direct excitation of the fast mode. The data for two detectors are plotted with different vertical scales. The fitted parameters are $\epsilon(\text{prism})=2.3$; $\epsilon(\text{MgF}_2)=1.94$; $\epsilon(\text{Ag})=(-14.5, 0.4)$; $d(\text{Ag})=47\text{ nm}$; $d(\text{MgF}_2)=300\text{ nm}$; the same root-mean-square roughness on both metal interfaces ($\delta_{44}^2g_{44}=\delta_{33}^2g_{33}$) and partial positive cross correlation $\delta_3\delta_{4g_{34}}=\delta_{4g_{44}}^2/4$.

DATA ANALYSIS

We apply now the general result [Eqs. (6a)–(6d)] to our particular geometry. We note first that in the experiment \mathbf{k}_{sc} is fixed and corresponds either to \mathbf{k}_f (fast-mode detector) or to \mathbf{k}_s (slow-mode detector). Furthermore, the incident light is p polarized, so that in the region where

$$I_f(k_I) \cong |\epsilon_4 - \epsilon_3|^2 \delta_{44}^2 g_{44}(\Delta \mathbf{k}) |E_z^p(k_f, z_4^+) E_z^p(k_I, z_4^-)|^2 + |\epsilon_3 - \epsilon_2|^2 \delta_{33}^2 g_{33}(\Delta \mathbf{k}) |E_z^p(k_f, z_3^+) E_z^p(k_I, z_3^-)|^2 + 2 \text{Re}[(\epsilon_4 - \epsilon_3)(\epsilon_3 - \epsilon_2)^* \delta_3 \delta_{4g_{34}}(\Delta \mathbf{k}) E_z^p(k_f, z_4^+) E_z^p(k_I, z_4^-) (E_z^p)^*(k_f, z_3^+) (E_z^p)^*(k_I, z_3^-)] \quad (9)$$

with a similar expression for $I_s(k_I)$. In deriving Eq. (9) we ignored contribution to scattered intensity from the prism-MgF₂ interface [$\zeta_2(\mathbf{x})=0$]. The reason for doing so is that the contribution of a rough interface to the scattering cross section is proportional to $|(\epsilon_i - \epsilon_{i-1})|^2$ and this is much smaller for MgF₂-prism interface than for the two other interfaces.

A few remarks are in order regarding Eq. (9). The first two terms in Eq. (9) are individual contributions from two interfaces, and the third one arises from the cross correlation between the profiles of the two rough surfaces. Since the two interfaces in question bound a rather thin (~ 40 -nm) silver layer, we expect nonzero contributions from this term. We further note that the contribution of each interface to the “conversion rate” by which we mean here the radiation from one of the modes while the other is driven directly is proportional to the overlap of the electric fields associated with these two modes at this particular interface.

$k_I=k_s$ or $k_I=k_f$ s -polarized scattering can be ignored. Moreover $\mathbf{k}_I \cdot \mathbf{k}_{\text{sc}}=0$ for our experimental geometry [see Fig. 2(b)]. We have then

$$I_f(k_I) \cong \left| \sum_{i=2}^n (\epsilon_i - \epsilon_{i-1}) \zeta_i(\Delta \mathbf{k}) \times E_z^p(k_f, z_i^+) E_z^p(k_I, z_i^-) \right|^2, \quad (7a)$$

where $\Delta \mathbf{k}=\mathbf{k}_f - \mathbf{k}_I$ for the fast-mode detector, and

$$I_s(k_I) \cong \left| \sum_{i=2}^n (\epsilon_i - \epsilon_{i-1}) \zeta_i(\Delta \mathbf{k}) \times E_z^p(k_s, z_i^+) E_z^p(k_I, z_i^-) \right|^2, \quad (7b)$$

where $\Delta \mathbf{k}=\mathbf{k}_s - \mathbf{k}_I$ for the slow-mode detector.

We note that the preceding equations still involve deterministic profiles $\zeta_i(\mathbf{x})$. Thus for random roughness, we assume that the diameter of the laser spot is much larger than the correlation lengths of the surface roughnesses, so we average Eqs. (7a) and (7b) over an ensemble of realizations of $\zeta_i(\mathbf{x})$. This will involve correlation moments $\langle \zeta_i(\mathbf{k}) \zeta_j^*(\mathbf{k}) \rangle$. Since $\zeta_i(\mathbf{x})$ is a stationary stochastic process (translational symmetry is preserved in the statistical sense), these moments satisfy the following relations:²⁰

$$\langle \zeta_i(\mathbf{k}) \zeta_j^*(\mathbf{k}) \rangle = A \delta_i \delta_j g_{ij}(|\mathbf{k}|), \quad (8) \\ |g_{ij}(k)| \leq [g_{ii}(k) g_{jj}(k)]^{1/2},$$

where δ_i is the root-mean-square roughness amplitude $\delta_i^2 = \langle \zeta_i^2(\mathbf{x}) \rangle$ and A is the illuminated surface area. The averaging leads to

Equation (9) was used to fit the data of Figs. 4 and 5. The $E(k, z)$ factors were calculated using the exact formalism that involves the multiplication of a set of 2×2 matrices (see Ref. 21). The fitting was done in two steps. First, the thickness of MgF₂ and Ag films, and the dielectric constant of silver were determined by fitting the position and the width of the dominant features in the data for each of the detectors. These features correspond to the process in which an excited SPP scatters 90° away from the original direction with no change in the magnitude of k , (i.e., fast-to-fast and slow-to-slow scattering). Secondly, the roughness parameters (assumed $\Delta \mathbf{k}$ independent) were used to fit the remaining features of the data. The best fit (Fig. 5) was obtained with $\delta_{44}^2 g_{44} = \delta_{33}^2 g_{33} = 4(\delta_3 \delta_{4g_{34}})$ that is with the same root-mean-square roughness amplitude on two interfaces and the partial positive cross correlation. The partial positive cross correlation means that the two metal-film interfaces parallel each other to a certain degree. These parameters

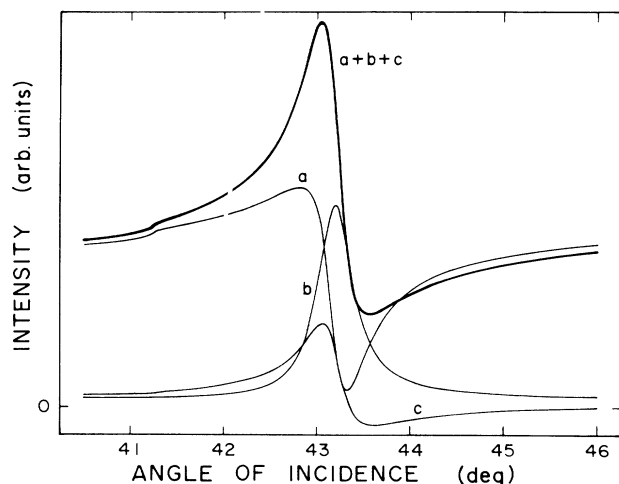


FIG. 6. The theoretical fit to the response of the slow-mode detector in the region where the fast mode is driven directly. The curves labeled *a*, *b*, and *c* represent, respectively, contribution from Ag-MgF₂, Ag-vacuum interfaces, and the interference term (cross correlation). Fit parameters are listed in the caption to Fig. 5.

reproduce the relative strength and angular dependence of the fast-to-slow conversion process, but underestimate the strength of the reverse process (slow to fast). We believe that this is an experimental artifact due to scattering of the incident laser beam on the edge of the prism, since the excitation angle for the slow mode was very close to the edge of the prism at 83°.

We do not quote here the absolute values of the roughness parameters. In order to obtain these, one would have to make absolute intensity measurements or relax the assumption of Δk independence of *g* factors in Eq. (9), and then try to fit the experimental data with some assumed Δk dependence of the *g* factors. We feel that the inherent difficulty of absolute intensity measurements of scattered light, and the fact that the exact functional form of the *g*(Δk) factors is always unknown would make such an undertaking questionable at best.

Figure 6 shows explicitly the contribution of each term in Eq. (9) to the total scattering cross section for the slow-to-fast conversion process. Note that the overall line shape is determined by all three terms, since the contribution of the cross-correlation term (interference effect) is comparable to the direct emission from the two interfaces.

DISCUSSION

Experimental data presented here clearly demonstrate that even on metal films that are not intentionally roughened, the roughness-induced mode conversion does

indeed occur. By applying a standard theoretical treatment (generalized to an arbitrary planar stack) that treats roughness in the first-order approximation we obtained a rather simple physical picture of the mode-conversion process. The salient points of this picture are as follows. The scattering of, say, mode *A* into mode *B* occurs on each rough interface of the stack with the rate determined by roughness parameters and the intensity of the electric field of a scattering mode *A* at this interface. If the excited mode *B* is radiative, emission will be proportional to the intensity of the electric field this mode would have if it were excited by radiation from outside the stack. The total emission by a particular mode is the sum of emissions from all interfaces modified by interference terms if roughnesses are correlated. Our experiment confirms that the theory is sufficiently accurate.

We would like to conclude with a few remarks regarding light-emitting tunnel junctions (LETJ). We note first that real-world structures are unavoidably rough; thus, in view of our results roughness-induced scattering has to be included in the full theory of emission from such structures, even if the geometry is such that it allows direct radiative decoupling of some of the modes (prism, grating). In fact, the calculations¹⁰ assuming smooth interfaces failed to account for the spectral distribution observed experimentally for LETJ fabricated on a prism coupler.¹⁰ We note that the formalism sketched in the present paper could easily be utilized in the more realistic (i.e., including roughness) LETJ calculations. The only difference between the situation considered in this paper and the LETJ is the location of the current source. We assume a source external to the stack, while in LETJ the source is inside the stack. The remaining parts of the model still apply. Specifically, the emission by a particular radiative mode will be determined by a sum of direct emission process *and* the conversion processes [Eq. (6)] occurring at all rough interfaces with each interface *z_i* emitting with the efficiency determined by $E(k, \omega z_i)$, i.e., with the same efficiency that an external source generates fields inside the structure. This feature of the theory implies that at least in theory a structure consisting of a metal film, tunneling spacer, and an optically transparent electrode decoupled through the prism, should improve efficiency of LETJ provided that the source current is localized in the spacer as has been in fact suggested.²²

ACKNOWLEDGMENTS

This work was supported by the Department of Energy, Grant No. DE-FG03-85ER45196. One of us (S.U.) would like to acknowledge support by the U.S. National Science Foundation and the Japan Society for Promotion of Science through the U.S.-Japan Cooperative Science Program. J.C.H. would like to thank the Alfred P. Sloan Foundation for support.

*Present address: IBM, Almaden Research Center, San Jose, CA 95120.

¹*Surface Enhanced Raman Scattering*, edited by R. K. Chang and T. E. Furtak (Plenum, New York, 1982).

²Y. Y. Chen, W. P. Chen, and E. Burstein, *Phys. Rev. Lett.* **36**,

1207 (1976).

³B. Pettinger, A. Tadjeddine, and D. M. Kolb, *Chem. Phys. Lett.* **66**, 544 (1979).

⁴S. Ushioda and Y. Sasaki, *Phys. Rev. B* **27**, 1401 (1983); **29**, 2309 (1984).

- ⁵K. Kurosawa, R. M. Pierce, S. Ushioda, and J. C. Hemminger, *Phys. Rev. B* **33**, 789 (1986).
- ⁶C. K. Chen, T. F. Heinz, D. Richards, and Y. R. Shen, *Phys. Rev. Lett.* **46**, 1010 (1981).
- ⁷J. Lambe and S. L. McCarthy, *Phys. Rev. Lett.* **37**, 923 (1976).
- ⁸J. R. Kirtley, T. N. Theis, J. C. Tsang, and D. J. DiMaria, *Phys. Rev. B* **27**, 4601 (1983).
- ⁹E. Kretschmann and H. Raether, *Z. Naturforsch.* **23a**, 2135 (1968).
- ¹⁰S. Ushioda, R. M. Pierce, and J. E. Rutledge, *Phys. Rev. Lett.* **54**, 224 (1985).
- ¹¹R. W. Gruhlke, W. R. Holland, and D. G. Hall, *Phys. Rev. Lett.* **56**, 2838 (1986).
- ¹²M. G. Weber and D. L. Mills, *Phys. Rev. B* **32**, 5057 (1985).
- ¹³C. E. Reed and J. Giergiel (unpublished).
- ¹⁴E. Kröger and E. Kretschmann, *Z. Phys.* **237**, 1 (1970).
- ¹⁵B. Laks and D. L. Mills, *Phys. Rev. B* **20**, 4962 (1979).
- ¹⁶D. L. Mills and A. A. Maradudin, *Phys. Rev. B* **12**, 2943 (1975).
- ¹⁷P. Bousquet, F. Flory, and P. Roche, *J. Opt. Soc. Am.* **71**, 1115 (1981).
- ¹⁸C. E. Reed, J. Giergiel, J. C. Hemminger and S. Ushioda *Phys. Rev. B* (to be published).
- ¹⁹*Electrodynamics of Continuous Media*, L. D. Landau and E. M. Lifshitz (Pergamon, New York, 1960).
- ²⁰See, for example, A. A. Maradudin, in *Surface Polaritons*, edited by V. M. Agranovich and D. L. Mills (North-Holland, Amsterdam, 1982), pp. 405–510.
- ²¹C. E. Reed, J. Giergiel, and S. Ushioda, *Phys. Rev. B* **31**, 1873 (1985).
- ²²D. L. Mills, M. Weber, and B. Laks, *Tunneling Spectroscopy*, edited by P. K. Hansma (Plenum, New York, 1982), Chap. V, pp. 121–152.